

Molecular-Dynamics Simulation of a Glassy Polymer Melt: Rouse Model and Cage Effect

C. Bennemann, J. Baschnagel, W. Paul*, and K. Binder

*Institut für Physik, Johannes-Gutenberg Universität,
Staudinger Weg 7, D-55099 Mainz, Germany*

Abstract

We report results of molecular-dynamics simulations for a glassy polymer melt consisting of short, linear bead-spring chains. The model does not crystallize upon cooling but exhibits a glassy slowing down. The onset of this slowing down is brought about by the dense packing in the melt. It was shown in previous work that this onset is compatible with the predictions of the mode coupling theory of the glass transition. The physical process of “caging” of a monomer by its spatial neighbors leads to a distinct two step behavior in scattering functions and particle mean square displacements. In this work we analyze the effects of this caging process on the Rouse description of polymer melt dynamics. The Rouse model is known, both from experimental and simulational work, to be a reasonable description of the dynamics of short chains in the melt. We show that the Rouse description is applicable for length and time scales above the typical scales for the caging process and that the typical time scale of the Rouse model reflects the onset of freezing as described by mode coupling theory. The Rouse modes are eigenmodes of the chains also in the supercooled state, and the relaxation times of the modes exhibit the same temperature dependence as the diffusion coefficient of the chains. The decay of the mode correlation functions is stretched and depends on the mode index. Therefore, there is no time-mode superposition of the correlation functions. However, they exhibit a time-temperature superposition at late times. At intermediate times they decay in two steps for temperatures close to the dynamical critical temperature of mode coupling theory. The monomer displacement is compared with simulation results for a binary LJ-mixture to point out the differences which are introduced by the connectivity of the particles.

PACS: 61.20.Ja,64.70.Pf,61.25.Hq,83.10.Nn

accepted by *Comp. Theo. Poly. Sci.*

I. INTRODUCTION

In 1953 P. E. Rouse proposed a simple model to describe the dynamics of a polymer chain in dilute solution [1]. The model considers the chain as a sequence of Brownian particles which

*To whom correspondence should be addressed. Email: Wolfgang.Paul@uni-mainz.de

are connected by entropic harmonic springs. Being immersed in a structureless solvent the chain experiences a random force by the incessant collisions with the (infinitesimally small) solvent particles. The random force is assumed to act on each monomer separately and to create a monomeric friction coefficient. The model therefore contains chain connectivity, a local friction and a local random force. All non-local interactions between monomers distant along the backbone of the chain, such as excluded-volume or hydrodynamic interactions, are neglected. In dense melts, where both interactions are screened, the Rouse model was shown to describe the viscoelastic properties of short chain melts [2,3,4]. For the polyethylene melts studied in [4] it was also shown by neutron spin-echo experiments [5,6] and computer simulations [7,8] that the conformational dynamics can be reasonably well described by the Rouse model on length scales below the radius of gyration and time scales below the longest relaxation time of the chains (Rouse time). However, by construction (see section II), it can also only be applicable on length scales above the statistical segment length, b , of the chains and on time scales larger than $b^2\zeta/k_B T$, where ζ is the monomer friction coefficient. On length scales below the statistical segment length local stiffness effects due to the intramolecular potentials become important and there are several suggestions in the literature how to incorporate those into a modified Rouse model [9,10].

For a short chain polymer melt undergoing a glass transition it is also well established that the dramatic increase in relaxation times observable for instance in the viscoelastic response can be accounted for within the Rouse model by fitting a temperature dependent monomer friction coefficient in the form of a Vogel-Fulcher-Tammann (VFT) law [2,4]

$$\zeta(T) = \zeta_\infty \exp \left[\frac{E}{T - T_0} \right] . \quad (1)$$

The extrapolated temperature of divergence, T_0 , in this law (complete structural arrest) together with the (also extrapolated) vanishing of the excess configurational entropy of the glass with respect to the crystal (Kauzmann paradox [11]) lead to theories assuming an underlying phase transition for the glassy freezing [12,13,14]. Especially the Gibbs-DiMarzio theory for polymers is capable of reproducing many phenomenological properties of the polymer glass transition, the prediction of a vanishing configurational entropy, however, could be shown to arise from too crude approximations in calculating the high temperature limit [15]. The physical significance of these extrapolated singularities is therefore questionable.

The VFT law has one further characteristic feature. There exists a temperature region, where the behavior of the viscosity turns over from a gradual high temperature increase upon lowering the temperature to a very steep increase in the supercooled region approaching the viscosimetric glass transition temperature T_g . In this temperature region a change in the physical relaxation mechanism occurs. At high temperatures the mean square displacement of the particles directly crosses over from short time ballistic to long time diffusive motion. In this crossover region a plateau regime intervenes where the particles are temporarily trapped in a cage formed by their neighbors until some thermally activated process leads to an escape from the cage. Experimentally, this two step process is best observed in intermediate scattering functions, and it is well established for all fragile to intermediate glass forming systems [16,17], i.e., those where the viscosity is describable by the VFT law, but is also observable for strong glass formers at very high temperatures [18] (where the viscosity follows an Arrhenius law).

Theoretically it is the mode coupling theory of the glass transition (MCT) [19,20,21] that focuses on this temperature region. In its idealized version (neglecting the activated processes that lead to an escape from the cage) it predicts an ergodic to non-ergodic transition at a dynamical critical temperature T_c , which phenomenologically seems to be the same as the inflection point in the VFT law (Fischer et al. in [17]) marking the center of the crossover region.

In this work we want to answer the question, how this two step relaxation process that is induced by the cage effect influences the Rouse model description of the dynamics of short chain polymer melts.

We have shown in previous work [22,23,24] that the two step relaxation process occurring in our model upon supercooling the system is compatible with the MCT predictions and have determined the dynamical critical temperature $T_c = 0.45$ and the exponent parameter $\lambda = 0.635$ governing the algebraic divergence of correlation times at this temperature in the idealized version of the MCT. In this work, we will analyze the conformational relaxation of the chains and their self-diffusion properties in the same temperature region in terms of the Rouse model.

Section II will introduce our simulation model and a short collection of results from the Rouse model for later reference. In section III we will then look at the behavior of the Rouse modes and section IV will focus on the self-diffusion properties of our model. Section V will present our conclusions.

II. SIMULATION MODEL AND THEORETICAL BACKGROUND

In this section we will give a short introduction to our simulation model and technique and then summarize some pertinent results from the analytic solution of the Rouse model. A more detailed description of our simulation model can be found in reference [22].

A. Simulation Model

Our simulation model consists of bead spring chains of length $N = 10$. All beads interact through a Lennard-Jones potential

$$U_{\text{LJ}}(r_{ij}) = 4\epsilon \left[\left(\frac{\sigma}{r_{ij}} \right)^{12} - \left(\frac{\sigma}{r_{ij}} \right)^6 \right], \quad (2)$$

which is truncated at $2 \times 2^{1/6}\sigma$ and shifted so as to vanish smoothly at that point. $\sigma = 1$ defines the length scale and $\epsilon = 1$ defines the temperature scale of our model. Bonded neighbors in a chain furthermore interact through a FENE potential

$$U_{\text{FENE}}(r_{ij}) = -15R_0^2 \ln \left[1 - \left(\frac{r_{ij}}{R_0} \right)^2 \right] \quad (3)$$

with $R_0 = 1.6$. The resulting equilibrium bond length is $l_0 = 0.96$. For a Lennard-Jones potential that is truncated in the minimum (soft spheres) this is the Kremer-Grest model

[25] for which it was shown that the conformational relaxation of short melt chains in the high temperature regime can be rather well described by the Rouse model [25,26]. Note, however, that the latter model (because of the strictly repulsive interaction between the monomers) does not yields physically reasonable equation of state for the polymer melt. Also the friction coefficient depends on temperature only weakly, unlike equation (1).

We performed Molecular Dynamics simulations in the canonical (NVT) ensemble using the Nosé–Hoover [27] thermostat. For each temperature, however, the equilibrium density is determined by an isobaric-isothermal (NpT) simulation before the canonical simulation was started. In this way we follow a constant pressure path upon cooling [24].

B. Rouse model

The Rouse model is defined through the following equation of motion for the repeat units of a polymer chain, \mathbf{r}_n being the position of the n -th effective monomer at time t ,

$$\zeta d\mathbf{r}_n(t) = \frac{3k_B T}{b^2} (\mathbf{r}_{n+1}(t) - 2\mathbf{r}_n(t) + \mathbf{r}_{n-1}(t)) dt + d\mathbf{W}_n(t), \quad (4)$$

where b is the statistical segment length of the chains and defines the length scale of the model, ζ is the monomer friction coefficient and the $d\mathbf{W}_n(t)$ denote random forces modeled as Gaussian white noise:

$$\langle dW_{n\alpha}(t)dW_{m\beta}(t') \rangle = \delta_{nm}\delta_{\alpha\beta}\delta(t-t')dt.$$

The Rouse modes are defined as the cosine transforms of position vectors, \mathbf{r}_n , to the monomers. For the discrete polymer model under consideration they can be written as [28]

$$\mathbf{X}_p(t) = \frac{1}{N} \sum_{n=1}^N \mathbf{r}_n(t) \cos \left[\frac{(n-1/2)p\pi}{N} \right], \quad p = 0, \dots, N-1. \quad (5)$$

The normalized time-correlation function of the Rouse modes is given by

$$\Phi_{pq}(t) = \frac{\langle \mathbf{X}_p(t) \mathbf{X}_q(0) \rangle}{\langle \mathbf{X}_p(0) \mathbf{X}_q(0) \rangle} = \exp \left[-\frac{t}{\tau_p(T)} \right], \quad p = 1, \dots, N-1 \quad (6)$$

with ($p, q \neq 0$)

$$\langle \mathbf{X}_p(0) \mathbf{X}_q(0) \rangle = \frac{b^2}{8N[\sin(p\pi/2N)]^2} \delta_{pq} \xrightarrow{p/N \ll 1} \frac{Nb^2}{2\pi^2 p^2} \delta_{pq} \quad (7)$$

and

$$\tau_p(T) = \frac{\zeta(T)b^2}{12k_B T[\sin(p\pi/2N)]^2} \xrightarrow{p/N \ll 1} \frac{\zeta(T)N^2 b^2}{3\pi^2 k_B T p^2}. \quad (8)$$

According to equations (6), (7) and (8) the Rouse modes should have the following properties: (1.) They are orthogonal at all times. (2.) Their correlation function decays exponentially. (3.) The normalized correlation functions for different mode indices, p , and

temperatures can be scaled onto a common master curve when the time axis is divided by $\tau_p(T)$. We will examine to what extent these properties are realized by the studied model. In order to do this comparison we use the following relations

$$b^2 = \frac{R^2}{N-1} \quad \text{and} \quad \frac{\zeta(T)b^2}{k_B T} = \frac{R^2}{N(N-1)D}, \quad (9)$$

where R^2 ($\simeq 12.3$) is the squared end-to-end distance, and D is the diffusion coefficient of a chain. The first relation holds because of the Gaussian chain statistics, which is well established in dense melts, and thus fixes the length scaling between the simulation and the Rouse model. Use of the second relation means the the diffusive behavior at late times is employed to fix the translation between the time scale of the simulation and the theory.

Using equation (5) for the Rouse modes the position vectors of the monomers can be written as

$$\mathbf{r}_n(t) = \mathbf{X}_0(t) + 2 \sum_{p=1}^{N-1} \mathbf{X}_p(t) \cos \left[\frac{(n-1/2)p\pi}{N} \right], \quad n = 1, \dots, N, \quad (10)$$

which implies for the mean square displacement of the n -th monomer

$$\langle [\mathbf{r}_n(t) - \mathbf{r}_n(0)]^2 \rangle = g_3(t) + 8 \sum_{p=1}^{N-1} \langle |\mathbf{X}_p(0)|^2 \rangle [1 - \Phi_p(t)] \cos^2 \left[\frac{(n-1/2)p\pi}{N} \right], \quad (11)$$

where $g_3(t) = \langle [\mathbf{R}_{\text{cm}}(t) - \mathbf{R}_{\text{cm}}(0)]^2 \rangle$ denotes the mean square displacement of the chains' center of mass. Note that only the orthogonality of the Rouse modes, i.e., $\Phi_{pq}(t) \sim \delta_{pq}$, enters the derivation of equation (11).

III. ROUSE MODES: TIME AND TEMPERATURE DEPENDENCE

For the Hamiltonian chosen for our simulation we find that the stiffness of the chains as for instance given by the characteristic ratio only weakly depends on temperature. We find $C_N = \langle R^2 \rangle / (N-1)l_0^2 = 1.52$ for $T = 1.0$ and $C_N = 1.46$ for $T = 0.46$. So there is a slight shrinking of the chains due to the non-bonded interactions. The assumption of Gaussian statistics for all intramolecular distances leads to equation (6) for the correlation function of the amplitudes of the Rouse modes. We find for our model [29] that the static cross correlations between different modes p and q are always two to three orders of magnitude smaller than the static autocorrelation of modes p , shown in Figure (1). We can see that the mode amplitudes are independent of temperature as could be expected from the behavior of the characteristic ratio. Their qualitative trend as a function of mode number is the same as for the Rouse prediction of equation (7). Quantitatively, however, already the second Rouse mode shows a small deviation from the Rouse prediction (full curve in Figure (1), which was plotted using the calculated value for the autocorrelation of mode $p = 1$ according to equation (7) using (9) to relate to quantities measured in the simulation). Up to mode $p = 6$ (this is the scale of a dimer) the behavior can be described by a power law with an effective exponent $x = 2.2$, whereas the small- p expansion of equation (7) with exponent $x = 2$ fails for $p > 3$. These deviations from the Rouse prediction stem from the fact that

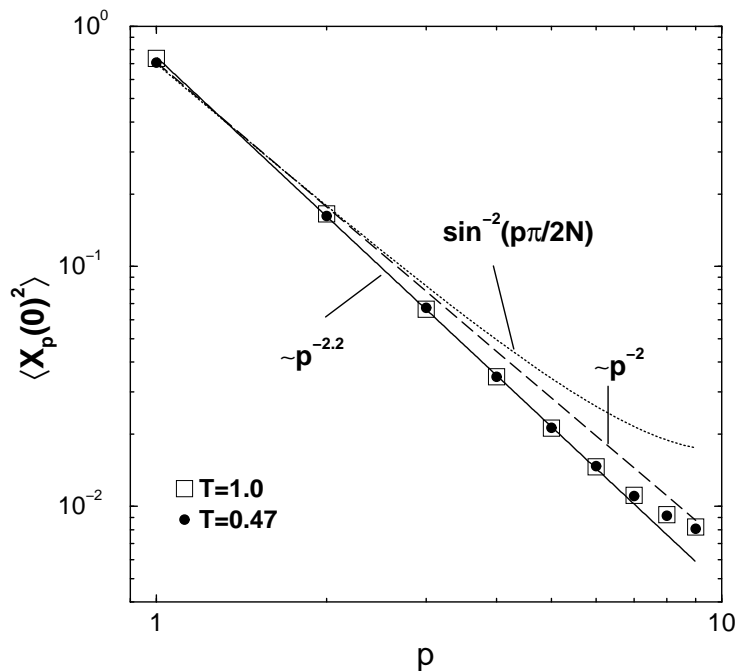


FIG. 1. Dependence of the initial correlation of the Rouse modes, $\langle \mathbf{X}_p^2(0) \rangle$, on the mode index p at $T = 0.47$ and $T = 1$. The theoretical expectations of the discrete [$\sim \sin^{-2}(p\pi/2N)$] and continuous ($\sim p^{-2}$) Rouse models are indicated as a dotted and a dashed line, respectively. In both cases, the prefactor was not adjusted, but calculated from the end-to-end distance ($R^2 \simeq 12.3$) according to equations (7) and (9). The solid line is a power law fit, $\langle \mathbf{X}_p^2(0) \rangle \sim p^{-x}$, with an effective exponent $x \simeq 2.17$.

the assumption of Gaussian distributed intramolecular distances breaks down on the length scale R/p connected with mode p , where R is the end to end distance of the chain. They depend on the details of the polymer model under investigation [7,30].

Let us now turn to the dynamics of the Rouse modes. In Figure (2) we show the dynamic autocorrelation function of the first Rouse mode as a function of scaled time. The time scale τ_1 is defined as the time value where the mode autocorrelation function has decayed to a value of $\phi_1(\tau_1) = 0.3$. According to equation (6) this should lead to a master plot showing a single exponential decay, when the autocorrelation function for different temperatures are compared. In Figure (2) we included all simulated temperatures from $T = 0.49$ to $T = 1.0$, and we can see that the time-temperature superposition principle is fulfilled nicely. The master curve can, however, not be described by a single exponential decay as is obvious from the figure. If the complete decay is included into a single exponential fit a law $\exp(-1.2t/\tau_1)$ is obtained. The prefactor of 1.2 in the argument of the exponential compensates for the 0.3 definition versus the e^{-1} definition of the relaxation time. If only the last 85% of the decay are included into the Kohlrausch-Williams-Watts fit ($A_p \exp\{-\ln(A_p/0.3)(t/\tau_1)^{\beta_p}\}$) with the amplitude A_p and the exponent β_p as fit parameters, this law gets a prefactor of $A_1 = 0.98$ and an exponent $\beta_1 = 0.98$, which is equal to one within our error bars. These two fit curves bracket the observed scaling function for scaled times below one.

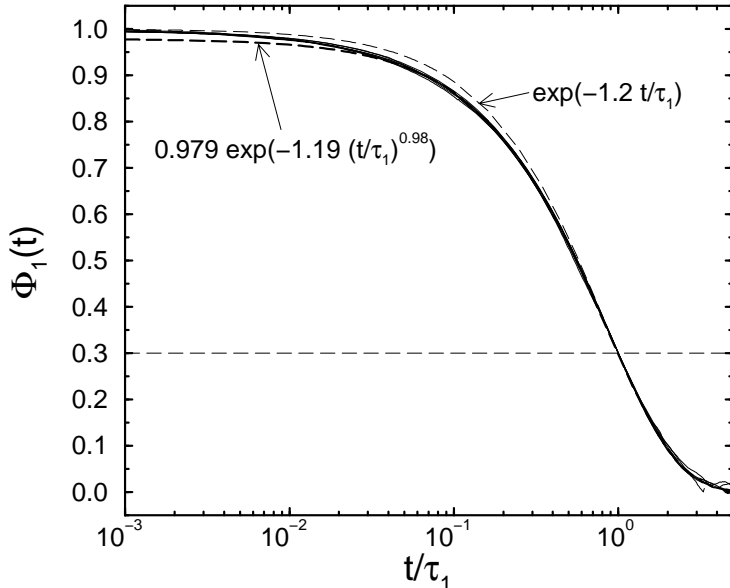


FIG. 2. Correlation function of the first Rouse mode, $\Phi_1(t)$, versus rescaled time t/τ_1 for seven different temperatures: $T = 0.49, 0.5, 0.52, 0.55, 0.6, 0.65, 0.7, 1$. The scaling time τ_1 is defined by $\Phi_1(\tau_1) = 0.3$ (dashed horizontal line). In addition, two exponential functions are shown. The upper (thin dashed line) has an amplitude of 1. It corresponds to the Rouse prediction [see equation (6)]. The lower (thick dashed line) is a fit for $0 \leq \Phi_1(t) \leq 0.85$.

The reason for the deviation of the scaling function from the single exponential decay is more obvious when we look at the mode autocorrelation function for higher p . As an example we show in Figure (3) the scaling plot for $p = 5$ for 5 temperatures ranging from $T = 0.47$ to $T = 1$. Here the time temperature superposition only works for the late stages of the decay (scaled times of about 0.5 and larger), the so-called α -process. The scaling range between the curves at different temperatures, however, increases upon lowering the temperature. The dashed curve in Figure (3) is the same exponential decay as in Figure (2). The master function for $p = 5$ is significantly stretched compared to the single exponential decay. Using again the last 85% of the decay for a fit to the Kohlrausch-Williams-Watts law, we get a stretching exponent of $\beta_5 = 0.81$ (dotted line). This stretching exponent for the α -relaxation is, however, independent of temperature in the shown temperature interval, which covers the high temperature liquid region ($T = 1.0$) as well as the supercooled fluid region ($T = 0.47$). This is the same result as was found in [30] for a Monte Carlo simulation of a polymer lattice model undergoing a glass transition, in contrast to the discussion in [31]. The decrease in the Kohlrausch exponent β_p upon supercooling that is predicted in that model calculation is not observed in our simulation. The stretching, however, strongly depends on mode number and the values for the exponent β_p for the different Rouse modes are collected in Table 1. This mode number dependence was also found in the lattice simulation [30] as well as an atomistic simulation of a polyethylene melt [7,8].

For scaled times below about 0.5, the α -scaling breaks down. For $p = 5$ we can resolve

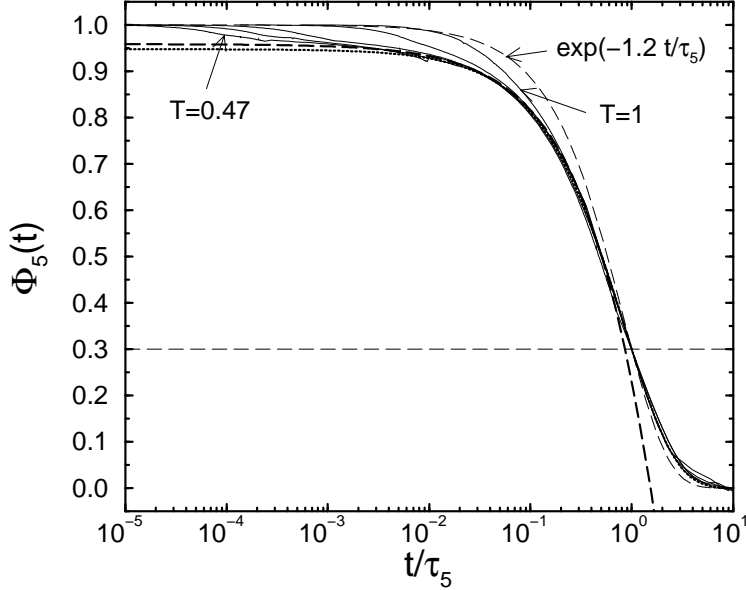


FIG. 3. Correlation function of the fifth Rouse mode, $\Phi_5(t)$, versus rescaled time t/τ_5 for five different temperatures: $T = 0.47, 0.49, 0.52, 0.7, 1$. The scaling time τ_5 is defined by $\Phi_5(\tau_5) = 0.3$ (dashed horizontal line). In addition, an exponential function (thin dashed line), a Kohlrausch function (dotted line), and a von-Schweidler fit (thick dashed line) are shown. The Kohlrausch function is given by $0.948 \exp[-1.15(t/\tau_5)^{0.87}]$ with $0 \leq \Phi_5(t) \leq 0.95$ as a fit interval. Using the von-Schweidler exponent $b = 0.75$ from the mode-coupling β -analysis [23] and fitting $\Phi_5(t)$ for $10^{-4} \leq t \leq 0.5$, the result for the von-Schweidler function is given by $0.959 - 0.815(t/\tau_5)^{0.75} + 0.086(t/\tau_5)^{1.5}$.

the development of a two step decay for temperatures $T \leq 0.7$ with an intervening plateau that increases in length upon cooling. This is the manifestation of the cage effect in the Rouse modes. The consequences of this caging for the structural relaxation behavior of our model was analyzed in detail in [23]. It was not observable for $p = 1$ because the amplitude of the plateau is too close to one in that case (even for $p = 9$ it is still larger than 0.9), but it leads to the discussed deviations from the single exponential decay. This plateau regime is called β -relaxation within mode coupling theory and the decay off the plateau should be describable by a von Schweidler-like law

$$\Phi_5\left(\frac{t}{\tau_5}\right) = f_5^c - B_1\left(\frac{t}{\tau_5}\right)^b + B_2\left(\frac{t}{\tau_5}\right)^{2b}, \quad (12)$$

where we included the first correction to the leading order in analogy to the predicted behavior of the incoherent scattering function [32]. We take the von Schweidler exponent $b = 0.75$ from our previous work [23] and fit the von Schweidler law to the data in the time interval $10^{-4} \leq t/\tau_5 \leq 0.5$ and obtain a very good description of the asymptotic scaling in this β -regime with the parameters f_5^c, B_1 and B_2 quoted in the caption of Figure (3).

Because of the mode number dependent stretching a time-mode superposition cannot be

expected to hold. In Figure (4a) we show the failure of the time-mode superposition for the

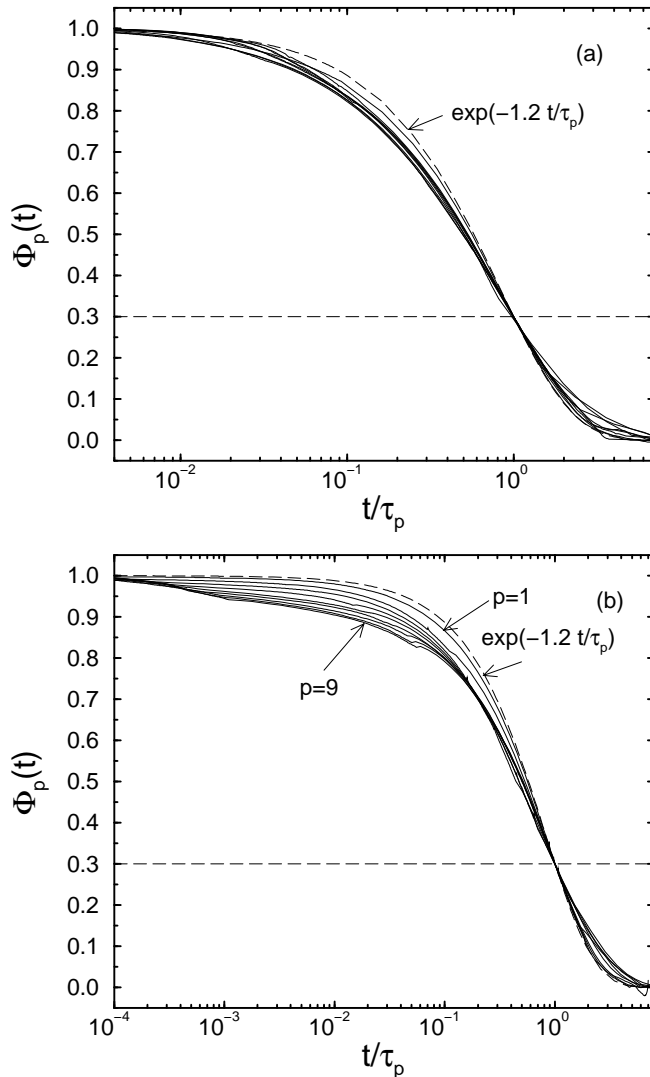


FIG. 4. Correlation functions of all nine Rouse modes, $\Phi_p(t)$, versus rescaled time t/τ_p for two different temperatures: $T = 1$ [normal liquid state of the melt; panel (a)], $T = 0.49$ [supercooled state close to $T_c = 0.45$ [23]; panel (b)]. The scaling time τ_p is defined by $\Phi_p(\tau_p) = 0.3$ (dashed horizontal line). In addition, an exponential function (thin dashed line) is shown.

high temperature liquid case ($T = 1$) and Figure (4b) shows the same for the supercooled state ($T = 0.49$). Here we can also observe the development of the β -plateau with increasing mode number with a plateau value of about 0.9 for $p = 9$.

When we look at the temperature dependence of the mode relaxation times τ_p within the Rouse model, equations (7) with (9) tell us that the quantity $\tau_p D/R^2$, where D is the center of mass diffusion coefficient and R^2 the squared end-to-end distance of the chains, should be independent of temperature. Figure (5) shows that this is indeed the case and that the dependence on mode index can be very well described by the Rouse prediction up to $p = 4$. The improved agreement with the Rouse model in comparison to the static

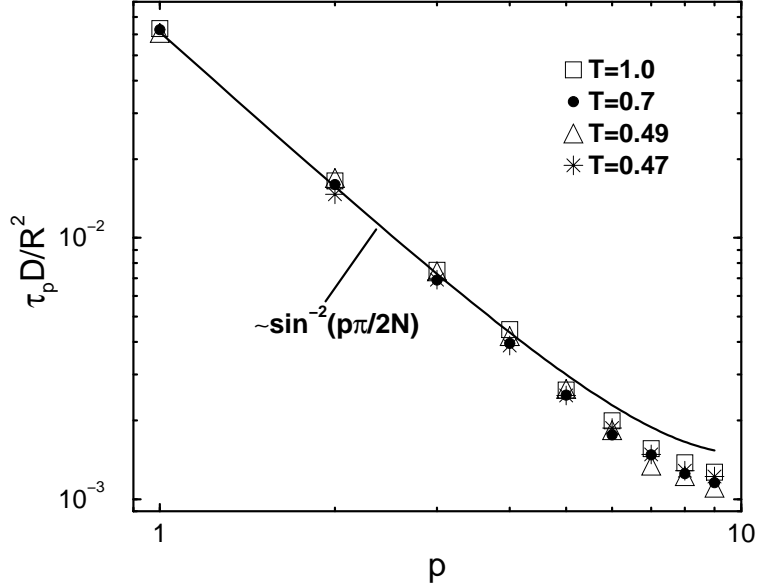


FIG. 5. Variation of the Rouse mode relaxation time with the mode index p for four different temperatures: $T = 0.47, 0.49, 0.7, 1$. The relaxation time τ_p is defined as the time value, at which the correlation function of the Rouse modes has decayed to 0.3, i.e., $\Phi_{pp}(\tau_p) = 0.3$. If $T < 0.49$, the decay of the function for the first mode is too slow to reach 0.3 within the simulation time. Therefore, only the results for $p \geq 2$ are shown for $T = 0.47$. As anticipated by equations (8) and (9), the temperature dependence of τ_p scales as $1/D$ (R is essentially temperature independent). The solid line is the prediction of the discrete Rouse model for the p -dependence of τ_p . The prefactor is $1.62 \times 1/12N(N-1)$. Contrary to Figure 1, an additional factor (i.e., 1.62) was necessary to shift the Rouse prediction onto the simulation data because the correlation functions do not exhibit a simple exponential decay so that the used definition of τ_p ($\Phi_{pp}(\tau_p) = 0.3$) can deviate from the Rouse definition ($\Phi_{pp}(\tau_p) = e^{-1}$) by a numerical constant.

behavior in Figure (1) suggests that the deviations from the conformational assumptions in the Rouse model are partially compensated by deviations from the dynamic assumptions going into the model, as they are manifest in the stretching of the modes.

In Figure (6) we finally analyze the temperature dependence of the mode relaxation times within the framework of the mode coupling theory of the glass transition. To this end, we plot the measured relaxation times double-logarithmically as a function of the distance to the mode coupling critical temperature $T_c = 0.45$ as determined for our model in [23]. For about one decade in the reduced temperature we observe an algebraic behavior as predicted for the α -relaxation time within MCT. For $T \leq 0.49$ deviations from the algebraic divergence at T_c occur, where ergodicity restoring processes that were neglected in the idealized MCT calculation start to become important. The exponent we observe is $\gamma_p = 1.83 \pm 0.02$, which is within the error bars equal to the exponent observed for the temperature dependence of the self-diffusion coefficient of the chains $\gamma_D \simeq 1.82$. The error bar for γ_p indicates the scattering between the fits to the different modes when fixing

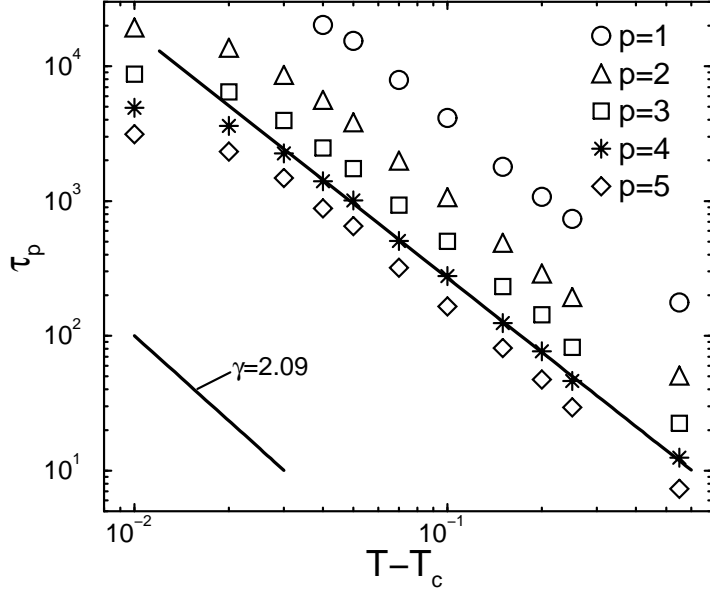


FIG. 6. Log-log plot of the Rouse relaxation time τ_p versus $T - T_c$ for the first five Rouse modes. τ_p is defined by $\Phi_{pp}(\tau_p) = 0.3$, and $T_c = 0.45$ is the critical temperature of mode-coupling theory (MCT) [23]. Additionally, two solid lines are shown: The lower one indicates the exponent expected from the MCT β -analysis, i.e., $\gamma = 2.09$ [23]. The other line through the data point for $p = 4$ represents a fit result for $0.49 \leq T \leq 1$, yielding $\gamma_p = 1.83 \pm 0.02$. Within the error bars, this exponent provides a reasonable fit not only for $p = 4$, but for all modes shown.

$T_c = 0.45$. The exponent is distinctly different from the $\gamma = 2.09$ obtained from a β -analysis of the incoherent scattering function in [23]. The agreement of the temperature dependence of an orientational correlation time as given by τ_1 and a translational correlation time definable by R^2/D was also found experimentally from a comparison of dielectric and pulsed-field gradient NMR data [33]. It also gave rise to the scaling observed in Figure (5). We can conclude from Figure (6) that all modes show a freezing transition at the same temperature $T_c = 0.45$ and with the same exponent γ_p in contrast to an analysis in [34] which, however, had to employ a frozen matrix assumption. If one treats matrix and probe chain dynamics self-consistently a unique freezing temperature is again obtained [35].

In order to interpret the difference in exponent between the incoherent scattering function and the conformational relaxation times of a chain as given by the Rouse modes, we have to keep in mind that the relaxation times at the mode coupling T_c do not actually diverge but stay finite. When we compare the temperature dependence of $\tau_q(T)/\tau_q(T_c)$ for a given momentum transfer q with the temperature dependence of $\tau_p(T)/\tau_p(T_c)$ for a given Rouse mode p , the latter quantity decays much slower with increasing distance $T - T_c$ due to the presence of connectivity correlations between monomers of the same chain.

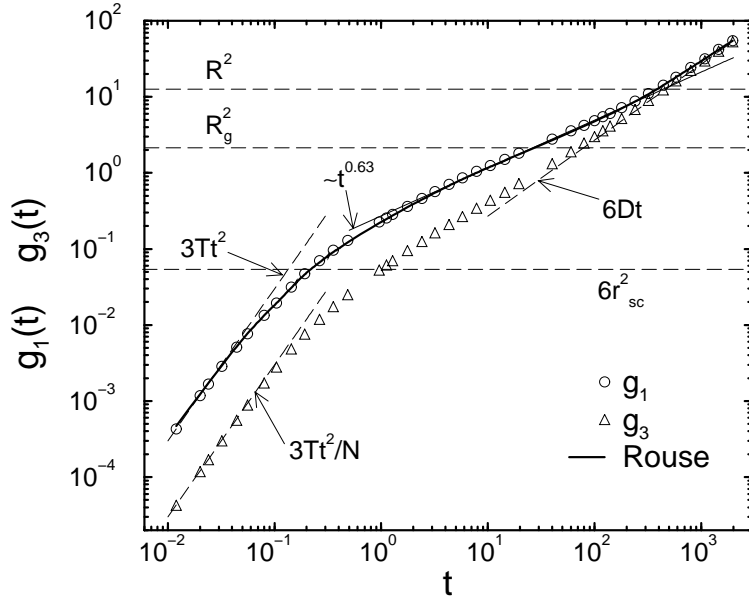


FIG. 7. Log-log plot of the mean-square displacements of an inner monomer, $g_1(t)$, and of the chains' center of mass, $g_3(t)$, versus time for $T = 1$. The thick solid line is the Rouse formula for $g_1(t)$ [see Eq. (11)]. The initial ballistic behaviors for $g_1(t)$ and $g_3(t)$, i.e., $g_1(t) = \langle v^2 \rangle t^2 = 3Tt^2$ and $g_3(t) = 3Tt^2/N$ ($\langle v^2 \rangle$: mean-square monomer velocity, $N = 10$: chain length), and the late time diffusive behavior are indicated as dashed lines. In addition, a power law fit $g_1(t) \sim t^x$ with an effective exponent $x \simeq 0.63$ is shown as a thin solid line. The dashed horizontal lines represent the end-to-end distance R^2 ($\simeq 12.3$; upper line) and the radius of gyration R_g^2 ($\simeq 2.09$; lower line), respectively.

IV. ROUSE MODEL AND MEAN SQUARE DISPLACEMENTS

In this section we want to analyze the translational behavior of central monomers of a chain, $g_1(t) = \langle [\mathbf{r}_{N/2}(t) - \mathbf{r}_{N/2}(0)]^2 \rangle$, and of the center of mass of a chain, $g_3(t)$, as a function of temperature. Figure (7) displays these functions in the high temperature case ($T = 1$). For short times both displacements are ballistic and equal to $\mathbf{v}^2 t^2 = 3Tt^2$ and $\mathbf{v}^2 t^2 / N$, respectively, in reduced units where $k_B = 1$ and the monomer mass is set to one. Then we see a crossover to a subdiffusive behavior in g_1 which is induced by the connectivity of the chains (Rouse mode dominated regime). The exponent in this regime is 0.63 instead of the Rouse prediction of 0.5, which is a deviation generally found in simulations and mostly attributed to the shortness of the chains leading to an early crossover from the Rouse mode regime to the long time free diffusion limit. This last regime is seen to occur, when the mean square displacements of the monomers are equal to the squared end-to-end distance of the chains. The center of mass displacement g_3 reaches the free diffusion limit at earlier times, namely when it is equal to the mean squared radius of gyration of the chains. The full line in Figure (7) proves in another way that the Rouse modes are eigenmodes of the chains. This curve is calculated from the mode autocorrelation functions using equation (11). As a

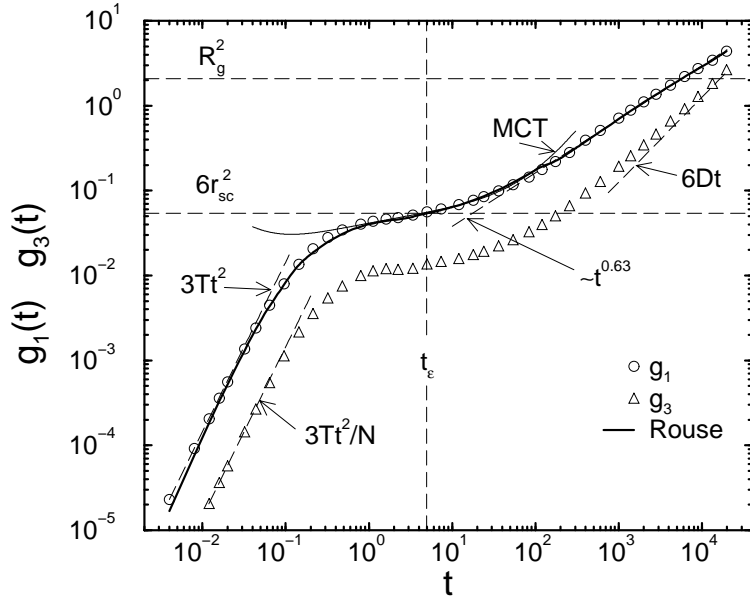


FIG. 8. Same as Fig. 7, but for $T = 0.48$. Additionally, the mode-coupling approximation in the β -relaxation regime, i.e., equation (13), is reproduced from Ref. [23]. The dashed horizontal lines indicate the plateau value, $6r_{sc}^2$, of equation (13) (lower line), the radius of gyration R_g^2 ($\simeq 2.09$; middle line) and the end-to-end distance R^2 ($\simeq 12.3$; upper line), respectively. The dashed vertical line indicates the β time scale t_ε from equation (13).

consistency check we exactly reproduce the monomer mean square displacement curve. We have to use all Rouse modes to obtain this exact agreement. If one only wants to describe the time dependence for $g_1(t) \geq R_g^2$, the first five Rouse modes suffice for our model. Also included in the Figure is a horizontal line at $6r_{sc}^2$ indicating the size of the next neighbor cage as obtained in [23]. For this displacement value we observe at high temperatures the crossover from the short-time ballistic motion to the short time diffusion and further the onset of the connectivity dominated regime. Both occur at the same distance scale, as the length scale of the non-bonded interaction, σ , and the bond length, l_0 , are approximately equal.

For the supercooled melt this picture changes qualitatively, as can be seen in Figure (8). For this temperature of $T = 0.48$ we were only able to propagate the chains for about two squared radii of gyration (after equilibration for about one order of magnitude longer in time). In the supercooled melt a plateau-like regime which extends for this temperature for about two decades in time intervenes between the short time ballistic regime and the connectivity dominated regime where the subdiffusive behavior again shows the exponent 0.63. This plateau is at the value of the cage size and it is centered on the β -relaxation time scale t_ε of MCT [23]. The MCT prediction for the mean squared monomer displacement $\langle(\Delta r)^2\rangle$, averaged over all monomers, for the β -regime is

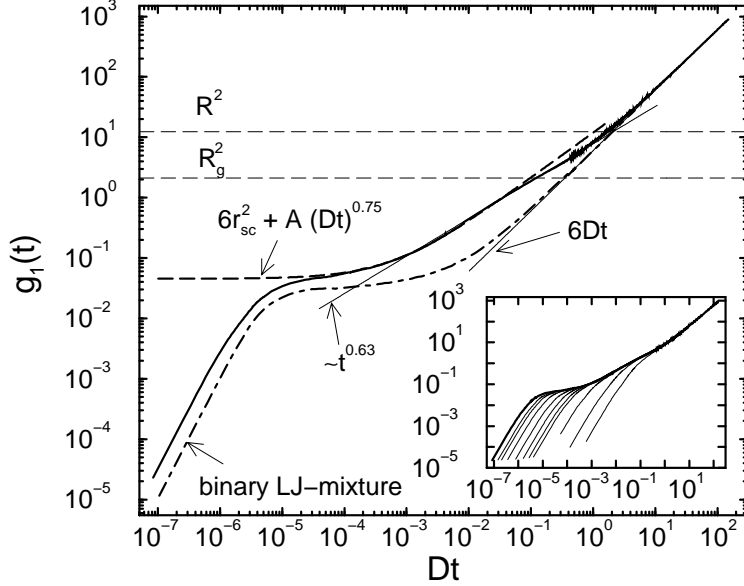


FIG. 9. Master curve of the mean-square displacement of an inner monomer $g_1(t)$ versus rescaled time Dt (D : diffusion coefficient of a chain). The master curve (= thick solid line in the inset and the main figure) is constructed from the temperatures $T = 0.48, 0.49, 0.5, 0.52, 0.55, 0.6, 0.65, 0.7, 1, 2, 4$ (from left to right in inset; the labels of the inset axes are identical to those of the main figure). The thick dash-dotted line is a master curve constructed from the simulation data of a binary Lennard-Jones mixture [36], including temperatures from $0.466 \leq T \leq 5$. Since $T_c \simeq 0.435$ for the binary mixture, but $T_c \simeq 0.45$ for the present polymer model, the lowest temperatures correspond to the same distance to the critical point, i.e., $T - T_c = 0.03$, in both cases. Additionally, two thin straight lines are shown, indicating a power law fit to the monomer displacement, $g_1(t) \sim t^x$ with $x \simeq 0.63$, and the late time diffusive behavior $6Dt$ which is common to the simple liquid and the polymer data. The thick dashed line is a fit to an effective von Schweidler law (see text). The dashed horizontal lines represent the end-to-end distance R^2 ($\simeq 12.3$; upper line) and the radius of gyration R_g^2 ($\simeq 2.09$; lower line), respectively.

$$g_1(t) \approx \langle (\Delta r)^2 \rangle = 6r_{\text{sc}}^2 - 6h_{\text{msd}} \left[\frac{t_0}{t_\varepsilon} \right]^a g(t/t_\varepsilon) - 6h_{\text{msd}} C_a \left[\frac{t_0}{t} \right]^{2a} - 6h_{\text{msd}} B^2 C_b \left[\frac{t_0}{t_\varepsilon} \right]^{2a} \left[\frac{t}{t_\varepsilon} \right]^{2b}. \quad (13)$$

The parameters $r_{\text{sc}}^2 = 0.009$, $h_{\text{msd}} t_0^a = 0.0045$, $t_\varepsilon = 4.933$, $a = 0.352$, $b = 0.75$, $B = 0.476$, $C_a t_0^a = -0.3$ and $C_b t_0^a = -0.25$ are taken from reference [23]. As was already discussed in that work, the MCT prediction for the β -regime for our model allows for a consistent description of the cage effect on the mean square monomer displacement. The MCT curve would predict a crossover from the breakup of the cage to the free diffusion of the particles, as no connectivity effects are included in the theory. For a polymer fluid, however, this behavior is altered and we obtain a crossover to the mode dominated regime, $t^{0.63}$, which is subdiffusive with a smaller exponent than the cage breakup described by the von Schweidler $t^{0.75}$ law (in leading order).

Figure (8) tells us also why an analysis of the caging process in a polymer melt within the framework of a theory developed for simple liquids can work at all. The typical distance traveled by a monomer at the plateau is of the order of 10^{-1} in units of the Lennard-Jones length scale which in turn is approximately equal to the bond length in our model. For this length scale connectivity effects are not yet felt by the monomers even in the high temperature regime shown in Figure (7). Only the late stage of the cage breakup (late β -process) and the structural relaxation (α -process) are influenced by the connectivity of the chains. It is also noteworthy that the analysis in terms of the Rouse modes works throughout the cage region as can be concluded from the full line in Figure (8), obtained in the same way as for Figure (7). Furthermore the caging process is not only observed in the monomer mean square displacement, but in the displacement of the center of mass of the chains as well.

The difference between a polymer melt and a simple liquid in the β - α crossover region is elucidated from a different angle in Figure (9). If we plot the mean square displacement for all temperatures as a function of time scaled by the center of mass diffusion coefficient at that temperature we obtain the set of curves displayed in the inset of Figure (9). The envelope master curve of this set of curves is shown in the main part of Figure (9) in comparison to the same master curve constructed for a binary Lennard-Jones fluid [36,37]. For large times the data for the two models have to agree by construction. But whereas for the Lennard-Jones fluid a direct crossover from the cage effect to the free diffusion occurs, the polymer exhibits the intervening connectivity dominated regime for length scales between the bond length, $l \approx 1$, and the end-to-end distance R . In this regime the observed mean square displacement curve drops below the MCT description, which is here displayed as an effective von Schweidler law $6r_1^2 + A_1(Dt)^{0.75}$, with $r_1 = 0.087$ and $A_1 = 11.86$. The same type of fit is possible for the displacement of the center of mass of the chains as is shown in Figure (10). The center of mass of a chain exhibits qualitatively the same crossover from the cage regime to the free diffusion regime as seen for the simple liquids. The fit values for the effective von Schweidler law in this case are $r_3 = 0.041$ and $A_3 = 2.68$.

V. CONCLUSIONS

We have shown in this work that the Rouse modes stay eigenmodes of the dynamics of short melt chains from the high temperature to the supercooled fluid state. They are orthogonal and for the smallest mode numbers they obey the predictions of the Rouse model for their static amplitudes. When the length scale probed by a mode is too short to allow for Gaussian distributed intramolecular distances on that scale, deviations from the static and dynamic scaling predictions occur. Nevertheless, when one uses the actual Rouse mode correlation functions to predict the time-dependent mean square displacements, one obtains perfect agreement with the simulation results.

The most important deviation from the Rouse model prediction is a mode number dependent stretching of the time autocorrelation function of the mode amplitude. This stretching is within our accuracy not temperature dependent for temperatures above the mode coupling critical temperature of our model, which were accessible for a dynamic analysis starting from equilibrated melts. We therefore have to conclude that it is not so much connected with the approach to the glass transition, but with deviations from the simple Rouse model due to

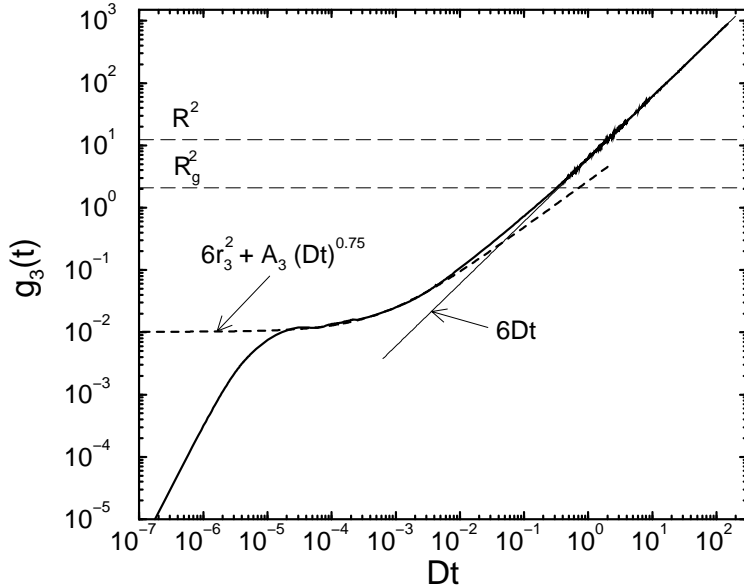


FIG. 10. Same as in Fig. 9, but for the mean-square displacement of the chains' center of mass $g_3(t)$. The master curve is constructed from the same temperatures as used for $g_1(t)$. The thin solid line indicates the late time diffusive behavior $6Dt$, and the thick dashed line is again a fit to an effective von Schweidler law (see text). The dashed horizontal lines represent the end-to-end distance R^2 ($\simeq 12.3$; upper line) and the radius of gyration R_g^2 ($\simeq 2.09$; lower line), respectively.

intramolecular stiffness and intermolecular interaction effects.

For temperatures in the supercooled fluid region the mode autocorrelation functions develop a clear two step decay similar to the behavior of the intermediate scattering function as discussed in [23] for the same model. The decay in the plateau region is compatible with the β -analysis following MCT presented earlier. Furthermore, the mode relaxation times follow the α -scaling behavior of MCT with the same dynamic critical temperature obtained from the intermediate scattering function. The exponent of the seeming algebraic divergence is the same as for the center of mass self-diffusion coefficient of the chains and different from the exponent seen in the intermediate scattering function. The difference can be understood in terms of additional correlations between monomers connected along the same chain, that are not included in the MCT, which was developed for simple liquids.

This connectivity leads to the Rouse prediction of a subdiffusive monomer displacement at intermediate times between the short time ballistic regime and the long time free diffusion limit. In the supercooled melt the cage effect, that leads to the discussed two step decays, intervenes between the short time ballistic motion of a monomer and the subdiffusive Rouse behavior. Therefore there is no direct crossover from the cage breakup to a free diffusion behavior as for simple liquids, but a crossover to the connectivity dominated regime with a smaller exponent than the von Schweidler exponent, which describes the cage breakup. Since the higher Rouse modes do not contribute to the center of mass displacement (which

is the zeroth Rouse mode), the center of mass of the chains exhibits qualitatively the same crossover from cage region to free diffusion as observed for simple liquids.

The whole applicability of the MCT to the supercooled polymer melt rests on the fact that the caging process occurs on a length scale of about one tenth of the bond length. On this scale the monomers just start to feel the connectivity to their neighbors and therefore only the late stages of the cage breakup and the structural relaxation are affected by the connectivity of the chains. The applicability of the Rouse model starts for length scales larger than the bond length and time scales of the order of the structural relaxation time of the melt.

ACKNOWLEDGMENT

We are indebted to Drs. W. Kob, M. Fuchs and I. Alig for helpful discussions. In the course of this work, we have profited from generous grants of simulation time by the computer center at the university of Mainz and the HLRZ Jülich, which are gratefully acknowledged, as well as financial support by the Deutsche Forschungsgemeinschaft under SFB262/D2.

-
- [1] P. E. Rouse, *J. Chem. Phys.* **21**, 1272 (1953).
 - [2] J. D. Ferry, *Viscoelastic Properties of Polymers* (Wiley, New York, 1980).
 - [3] M. Doi and S. F. Edwards, *The Theory of Polymer Dynamics* (Clarendon Press, Oxford, 1986).
 - [4] D. S. Pearson, L. J. Fetters, W. W. Graessley, G. ver Strate and E. von Meerwall, *Macromolecules* **27**, 711 (1994).
 - [5] D. Richter, L. Willner, A. Zirkel, B. Farago, L. J. Fetters and J. S. Huang, *Phys. Rev. Lett.* **71**, 4158 (1993).
 - [6] B. Ewen and D. Richter, in *Advances in Polymer Science*, (Springer, Berlin, 1997), Vol. 134, pp.1–129.
 - [7] W. Paul, G. D. Smith and D. Y. Yoon, *Macromolecules* **30**, 7772 (1997).
 - [8] W. Paul, G. D. Smith, D. Y. Yoon, B. Farago, S. Rathgeber, A. Zirkel, L. Willner and D. Richter, *Phys. Rev. Lett.* **80**, 2346 (1998).
 - [9] G. Allegra, *J. Chem. Phys.* **68**, 3600 (1978); G. Allegra and F. Ganazzoli, *J. Chem. Phys.* **74**, 1310 (1981).
 - [10] R. G. Winkler, P. Reineker and L. Harnau, *J. Chem. Phys.* **101**, 8119 (1994); L. Harnau, R. G. Winkler and P. Reineker, *J. Chem. Phys.* **102**, 7750 (1995); L. Harnau, R. G. Winkler and P. Reineker, *J. Chem. Phys.* **106**, 2469 (1997).
 - [11] W. Kauzmann, *Chem. Rev.* **43**, 219 (1948).
 - [12] G. Adam and J. H. Gibbs, *J. Chem. Phys.* **43**, 139 (1965).
 - [13] J. H. Gibbs and E. A. DiMarzio, *J. Chem. Phys.* **28**, 373 (1958); *ibid.* **28**, 807 (1958).
 - [14] G. S. Grest and M. H. Cohen, in *Advances in Chemical Physics*, Vol. 48, edited by I. Prigogyne and S. A. Rice (Wiley, New York, 1981), pp. 455–525.
 - [15] M. Wolfgardt, J. Baschnagel, W. Paul and K. Binder, *Phys. Rev. E* **54**, 1535 (1996).

- [16] Proceedings of the *2nd International Discussion Meeting on Relaxations in Complex Systems*, edited by K. L. Ngai, E. Riande and G. B. Wright [J. Non-Cryst. Solids **172-174**, (1994)].
- [17] Proceedings of the *3rd International Discussion Meeting on Relaxations in Complex Systems*, edited by K. L. Ngai, E. Riande and M. D. Ingram [J. Non-Cryst. Solids **235-237**, (1998)].
- [18] W. Kob, J. Horbach and K. Binder, in *Proceedings of the 8th Tohwa University International Symposium on Slow Dynamics in Complex Systems*, AIP Conference Proceedings, to appear 1999.
- [19] W. Götze, in *Liquids, Freezing and the Glass Transition*, edited by J. P. Hansen, D. Levesque and J. Zinn-Justin (North-Holland, Amsterdam, 1990), Part 1, pp. 287–503.
- [20] W. Götze and L. Sjögren, Rep. Prog. Phys. **55**, 241 (1992).
- [21] *Transport Theory and Statistical Physics*, edited by S. Yip, and P. Nelson (Marcel Dekker, New York, 1995), Vol. 24, No. 6–8.
- [22] C. Bennemann, W. Paul, K. Binder and B. Dünweg, Phys. Rev. E **57**, 843 (1998).
- [23] C. Bennemann, J. Baschnagel and W. Paul, *Molecular-Dynamics Simulation of a Glassy Polymer Melt: Incoherent Scattering Function*, accepted by *Eur. J. Phys. B*, cond-mat/9809335.
- [24] C. Bennemann, W. Paul, J. Baschnagel and K. Binder, *Investigating the influence of different thermodynamic paths on the structural relaxation in a glass forming polymer melt*, accepted by *J. Phys.: Condens. Matter*, cond-mat/9810020.
- [25] K. Kremer and G. S. Grest, J. Chem. Phys. **92**, 5057 (1990).
- [26] A. Kopf, B. Dünweg and W. Paul, J. Chem. Phys. **107**, 6945 (1997).
- [27] S. Nosé, Molec. Phys. **52**, 255 (1984); W. G. Hoover, Phys. Rev. A **31**, 1695 (1985).
- [28] P. H. Verdier, J. Chem. Phys. **45**, 2118 (1966).
- [29] C. Bennemann, Dissertation, University of Mainz 1998, unpublished.
- [30] K. Okun, M. Wolfgardt, J. Baschnagel and K. Binder, *Macromolecules* **30**, 3075 (1997).
- [31] R. F. Loring, J. Chem. Phys. **108**, 2189 (1998).
- [32] M. Fuchs, W. Götze and M. R. Mayr, Phys. Rev. E **58**, 3384 (1998).
- [33] M. Appel, G. Fleischer, J. Kärger, I. Chang, F. Fujara and A. Schönhals, *Colloid Polym. Sci* **275**, 187 (1997).
- [34] M. Rehkopf, V. G. Rostiashvili and T. A. Vilgis, *J. Phys. II France* **7**, 1469 (1997).
- [35] M. Rehkopf, Dissertation, University of Mainz 1998, unpublished.
- [36] W. Kob and H. C. Andersen, Phys. Rev. E **51**, 4626 (1995).
- [37] W. Kob, in *Annual Reviews of Computational Physics*, edited by D. Stauffer (World Scientific, Singapore, 1995), Vol. 3; pp. 1–43.

p	A_p	β_p
1	0.99	0.98
2	0.96	0.92
3	0.96	0.84
4	0.96	0.82
5	0.97	0.81
6	0.98	0.78
7	1.00	0.77
8	0.97	0.77
9	0.94	0.83

TABLE I. KWW amplitude A_p and stretching exponent β_p as a function of mode number. The KWW function was fitted to the last 85% of the decay. There is a systematic decrease of β_p with increasing mode number p , i.e. a systematic stretching of the modes. The exponent value for $p = 9$ seems to deviate from the trend, but also the KWW fit became worse for this high mode number.